*International Journal of Microwave and Wireless Technologies*

**cambridge.org/mrf**

# Improved feeds for log-periodic microstrip antenna arrays

Arjuna Muduli[1] and Rabindra K. Mishra[2]

[1]Department of ECE, Koneru Lakshmaiah Education Foundation, Vijayawada, Guntur 522502, Andhra Pradesh, India and [2]Electronic Science Department, Berhampur University, Berhampur 760007, Odisha, India

**Research Paper**

**Cite this article:** Muduli A, Mishra RK (2023). Improved feeds for log-periodic microstrip antenna arrays. *International Journal of Microwave and Wireless Technologies* **15**, 477–485. https://doi.org/10.1017/S1759078722000290

Received: 26 July 2021
Revised: 11 February 2022
Accepted: 14 February 2022
First published online: 23 March 2022

**Key words:**
End-fire antennas; log-periodic antennas; microstrip antennas

**Author for correspondence:**
Arjuna Muduli,
E-mail: arjunamuduli@gmail.com

**Abstract**

This note proposes a log-periodic microstrip antenna (LPMA), particularly after developing possible feed structures. The process develops an appropriate feed such that the LPMA can exhibit almost end-fire characteristics such as a log-periodic dipole antenna. The study simulated two LPMAs, one with five elements and the other with seven elements, followed by measurements on a five-element prototype. The five-element prototype LPMA with such a feed exhibits a bandwidth of 2.2–3 GHz. Over this band, radiation patterns remain consistent with a gain of 9.8 dBi. Simulated results follow the measured ones closely.

## Introduction

A log-periodic dipole antenna (LPDA) is a unidirectional form of a log-periodic antenna. It evolves from log-periodic-toothed trapezoidal antennas [1] by folding its two arms to make the included angle zero. Thus, while angles do not entirely describe an LPDA, it depends on angular coordinates. The initial development of an LPDA was by IsBell [2, 3]. Later, Carrel [4] proposed modification with a detailed study on LPDAs. Following this, LPDAs are well reported in the literature, particularly due to its directivity, wider bandwidth, and higher gain. The physical design of LPDAs uses a constant scaling factor ($\tau$) between its successive elements and the distance between them. The electrical excitation of an LPDA requires feeding of progressive elements with 180° phase difference to realize broadband operation. End-fire radiation patterns characterize LPDAs [2–4].

Microstrip antennas, being inherently narrowband, are natural candidates for adopting this concept for broadband operation. In [5], a simple coplanar microstrip series feeding network excites log periodically scaled patch elements. It includes a model that predicts input impedance and radiation patterns as a function of frequency. An experimental study on inset-fed rectangular and triangular microstrip arrays is available in [6]. In [7], a quasi-log-periodic antenna simulation is available. It uses square patches with an inset feed for impedance matching. It achieves a modest bandwidth. A single-layer log-periodic microstrip antenna (LPMA) with proximity-coupling to the feed line gives around 4 GHz bandwidth with 10.3 dBi gain [8]. In all these cases, the pattern is in the broadside direction, unlike LPDA.

Over the last decade, most of the reported work employing log-periodic principle has been on planar LPDAs. With printed planar helical dipoles as elements, the authors of [9] obtained a compact LP antenna with 4 GHz bandwidth and gain better than 5.73 dBi. For size reduction, a Koch-dipole element is useful in LPDAs [10].

Similarly, the use of trapezoidal-dipole elements in planar log-periodic antennas results in an operating band of 2–6 GHz [11]. The use of Sierpinski-dipole elements in log-periodic antenna arrays for operation in L and S bands results in size reduction of around 50% compared to LPDAs [12]. A low-profile (~0.047$\lambda$ at the lowest operating frequency) log-periodic array of cavity-backed slots fed by a meandered line [13] operates over a bandwidth from 6.9 to 17.4 GHz with good radiation characteristics. An eight-element log-periodic multiple-input multiple-output antenna for beam switching and dual-polarization characteristics [14] covers the ultra-wideband range with coupling isolation of more than 40 dB, the average peak gain of 6.5 dBi, and envelope correlation coefficient (ECC) < 0.005. An LPMA array with top parasitic loading using air gap is reported for broadcasting application [15] which can tune the bandwidth by adjusting the air gap.

A rigorous analysis for a series-fed electromagnetically coupled overlaid patch array is available [16]. The design presented is complex due to the multilayer structure involving shorting posts on each radiating element. Moreover, it concludes that uniform substrate thickness limits the bandwidth enhancement. In [17, 18], transmission line models estimate the input impedance of a series-fed LPMA. An LPMA with radiating part consisting of a pair of patches with a Koch curve structure placed vertically on both sides of the dielectric plate operates from 4 to 12 GHz [19]. A coplanar waveguide-fed LPMA with a defected ground plane for IoT applications, operating at 3.6 GHz, shows a gain of 9.36 dB [20]. However, the LPMA do not resemble the structure and electrical characteristics of an LPDA to a large extent. Particularly, they show a broadside pattern while mostly the patches are on two sides of the main feed line.



CAMBRIDGE UNIVERSITY PRESS

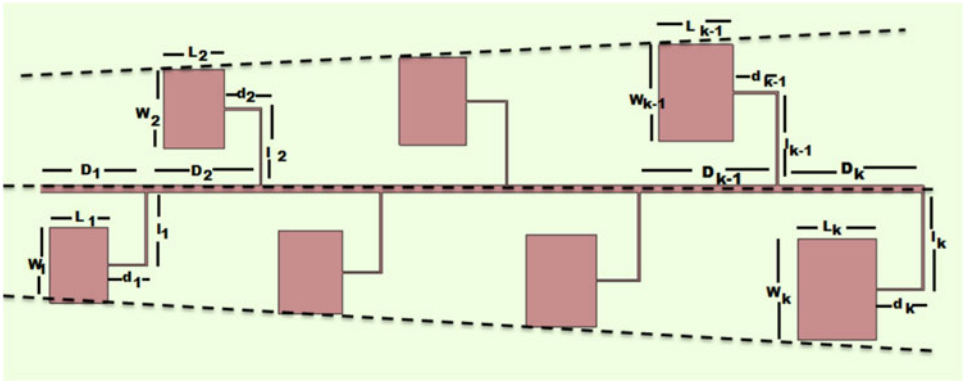


**Fig. 1.** Schematic diagram of the proposed LPMA.

**Table 1.** Design specifications

| Parameters | Literature [3]/proposed design |
|---|---|
| Frequency band | 2.03–2.73 GHz |
| Dielectric constant of substrate ($\varepsilon_r$) | 4.7 |
| Thickness of substrate ($h$) | 1.6 mm |
| Number of elements in the array ($N$) | 7 and 5 (minimum 3) |
| Scale factor ($\tau$) | 1.05 |

**Table 2.** Design parameters for LPMAs from [7] and the suggested method

| Frequency | | $L$, $W$ | $d$ | $l = D$ | $l$, $w_b$ |
|---|---|---|---|---|---|
| [7] | 2.03 | $L = W = 33.97$ | – | – | 10.8 |
| PA | | 34.16, 43.62 | 17.68 | 35.37 | 0.24 |
| [7] | 2.14 | $L = W = 32.35$ | – | – | 10.4 |
| PA | | 32.53, 41.54 | 16.84 | 33.68 | 0.22 |
| [7] | 2.24 | $L = W = 30.81$ | – | – | 9.8 |
| PA | | 30.98, 39.56 | 16.04 | 32.08 | 0.23 |
| [7] | 2.36 | $L = W = 29.34$ | – | – | 9.55 |
| PA | | 29.50, 37.68 | 15.28 | 30.55 | 0.24 |
| [7] | 2.48 | $L = W = 27.99$ | – | – | 9.0 |
| PA | | 28.10, 35.88 | 14.55 | 29.10 | 0.22 |
| [7] | 2.60 | $L = W = 26.61$ | – | – | 8.6 |
| PA | | 26.76, 34.17 | 13.86 | 27.71 | 0.22 |
| [7] | 2.73 | $L = W = 25.34$ | – | – | 8.2 |
| PA | | 25.48, 32.55 | 13.20 | 26.39 | 0.23 |

PA, proposed antenna in this paper.
Frequency in GHz, all other are in mm.
$L$, $W$, length and width; $w_b$, width of branch line.
In [7], $L = W$ and $l$ = inset depth for 50-Ω input impedance.
All values rounded off to two decimal points.

**Fig. 2.** Five-element prototype LPMA.

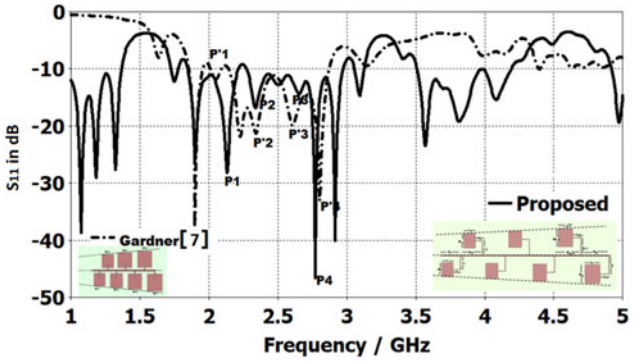


**Fig. 3.** Comparison of $S_{11}$-parameters for the two configurations (shown in the inset).

This paper shows that LPMAs can be realized like LPDAs with log-periodic characteristics using appropriate feed design irrespective of substrate thickness.

## Proposed LPMA design

### Number of elements

The proposed design assumes that each element will have the same percentage of bandwidth ($B$). The desired operating frequency range of the array extends from $f_1$ to $f_N$, with $N$ number of elements. The frequency scaling is according to the log-periodic principle (i.e. $f_k/f_1 = \tau^{1-k}$). Under these conditions, simple algebraic operations using the LP principle suggest rounding up $N$ (equation (1)) to the nearest upper integer gives the minimum number of elements:

$$N = \frac{\log(X - \tau) - \log(X - 1)}{\log(\tau)} \tag{1}$$

$$X = \frac{0.01\, B\tau}{\tau - 1} \tag{1a}$$

https://doi.org/10.1017/S1759078722000290 Published online by Cambridge University Press

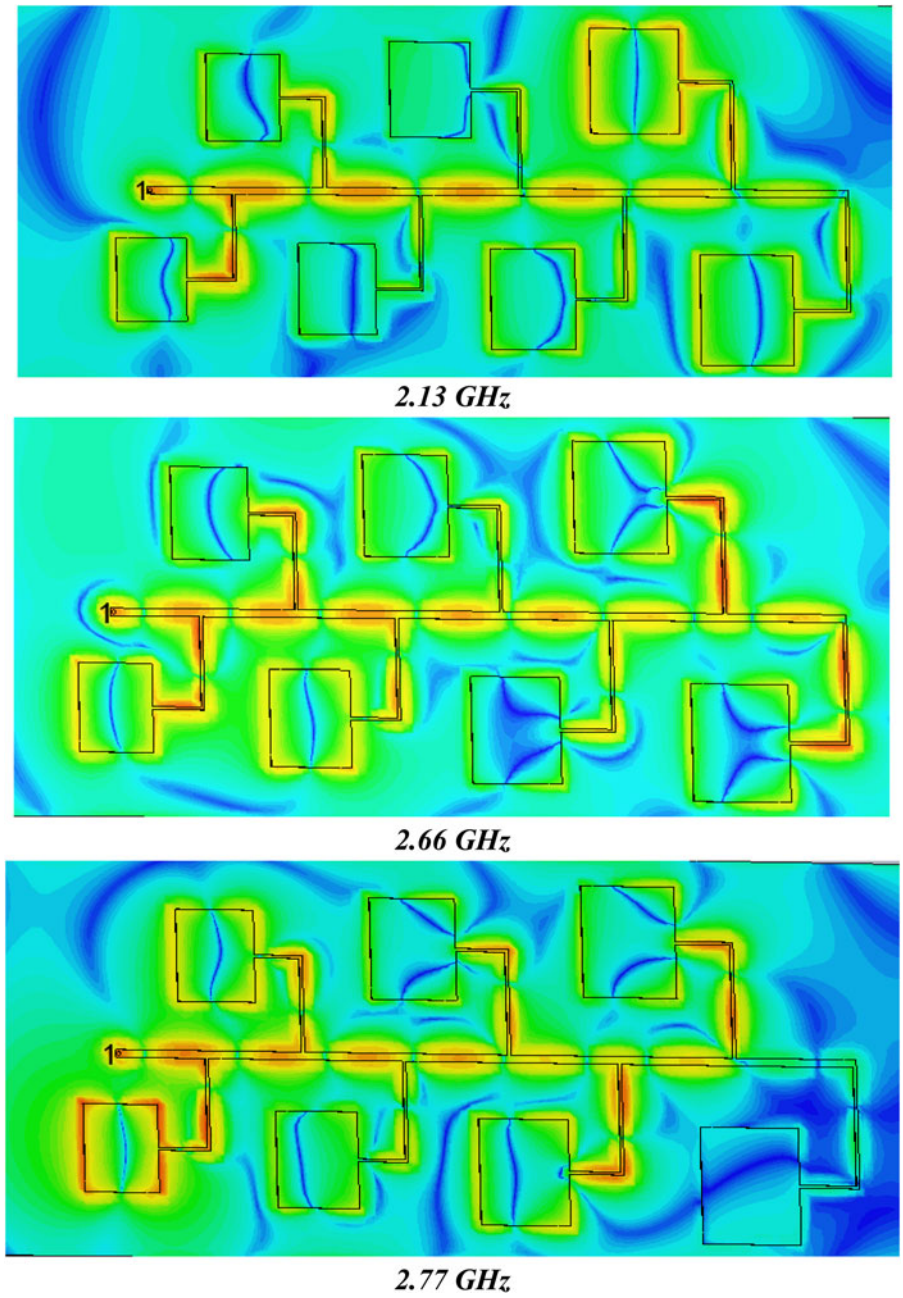


**Fig. 4.** Electric-field distribution in the proposed LPMA.

In the above equation, we assume $X$ as a variable and $\tau$ as the scaling factor of log-periodic antenna array.

### Choice of scaling factor ($\tau$)

A high-scale factor ($\tau$), spanning the design bandwidth, can result in fewer elements. The frequencies for which antenna elements are absent show unacceptable $S_{11}$. It results in discontinuous gain over the bandwidth. On the contrary, a small-scale factor requires many elements, leading to a long distance between the branch line and the open-end, which worsens the impedance characteristics. A conservative range of choice for $\tau$, following the LPDA design, is $1 \leq \tau \leq 1.05$.

### LP array element

The LPMA literature shows simple scaling of the physical length and width of patches. It neither considers the dependence of the patch length on the patch width nor justifies the negligence of this dependence in scaling. Of course, it is negligible in comparison with the operating wavelength. However, its contribution is evident in improving resonant frequency through effective dielectric constant. Although the lower operating frequencies mask the impacts of the effective dielectric constant to a large extent, they are not so at higher frequencies. As the width is independent of other dimensions, there is no problem in scaling it directly. A simple rearrangement of the scaling relation for width gives the formula for determining the width of the $k$th element of the array:

https://doi.org/10.1017/S1759078722000290 Published online by Cambridge University Press

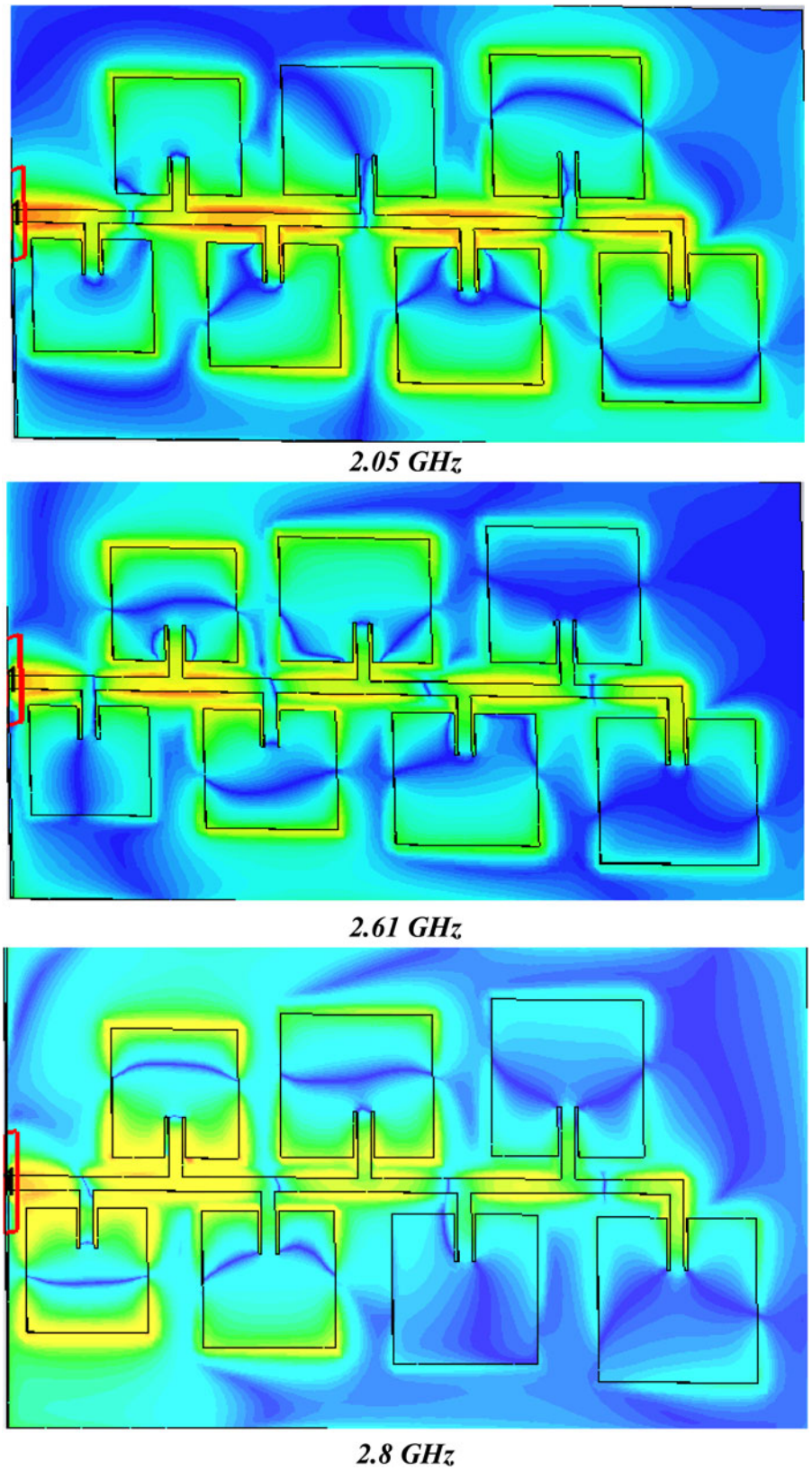


**Fig. 5.** Electric-field distribution in traditional LPMA of [7].

https://doi.org/10.1017/S1759078722000290 Published online by Cambridge University Press

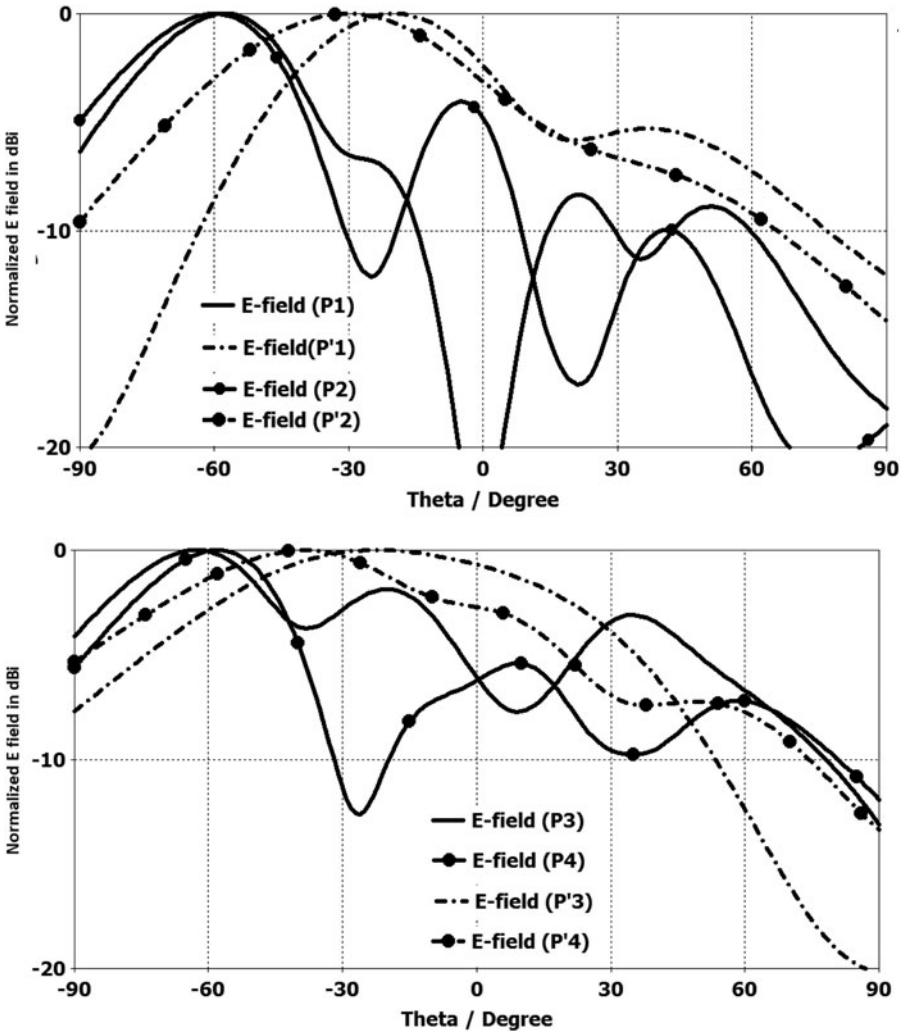


**Fig. 6.** Comparison of *E*-field patterns at resonant peaks, from left to right: *P*1, *P*′1 = 2.13, 2.05 GHz, *P*2 = *P*′2 = 2.34 GHz, *P*3, *P*′3 = 2.66, 2.61 GHz, *P*4, *P*′4 = 2.77, 2.8 GHz.

$$W_k = \frac{c\tau^{k-1}}{2f_1}\sqrt{\frac{2}{(\varepsilon_r+1)}} \tag{2}$$

As is well known, for a microstrip antenna, the effective dielectric constant, which is a function of its width, relates its physical length and electrical length. Accounting for the width through the effective dielectric constant, the length of the *k*th patch becomes

$$L_k = \tau^{k-1}(L_1 + 2\Delta L_1)\frac{\sqrt{\varepsilon_{eff,1}}}{\sqrt{\varepsilon_{eff,k}}} - 2\Delta L_k \tag{3}$$

At lower frequencies, which do not need stringent accuracy (up to two decimal points on a centimeter scale), one can use simple scaling as available in the literature [5–9, 17, 18].

## Element placement

### Mutual coupling reduction problem

In LPDAs, the electric dipoles are transversal to the direction of the feed [3, 4], and the pattern is end-fire. The end-fire pattern plays a major role in the significant mutual coupling among the dipole elements, leading to a broadband response. On the contrary, there are two dominating sources of mutual coupling reduction in LPMAs. The LPMA arrangement of the elements and their connection to the feeding line leads to short-circuiting off-resonant elements close to the feed point. Thus, there can be a substantial reduction in the mutual coupling, affecting the proper operation of the array. Moreover, in LPMAs, each element is equivalent to a pair of magnetic dipoles, and with the traditional feed [5–15], these dipoles are parallel to the main feed line. As seen later from simulation, this results in a radiation pattern more aligned to broadside (i.e. *H*-plane), reducing electrical interaction (i.e. mutual coupling) among elements which affects the broadband (i.e. log-periodic) nature of the LPMA.

### Compensating the mutual coupling reduction

The short-circuiting problem needs an impendence transformation to make it close to an open circuit for off-resonant points. For the *k*th array element, we use a branch line of length $3\lambda_{gk}/4$. For the end-fire (i.e. *E*-plane) pattern, we introduce a 90° bend near the antenna element in the derived feed line (Fig. 1), making its radiating edges transversal to the main feed. Alternative array elements are on the upper and lower sides of the mainline. It ensures out-of-phase excitation between two consecutive elements, essential

https://doi.org/10.1017/S1759078722000290 Published online by Cambridge University Press

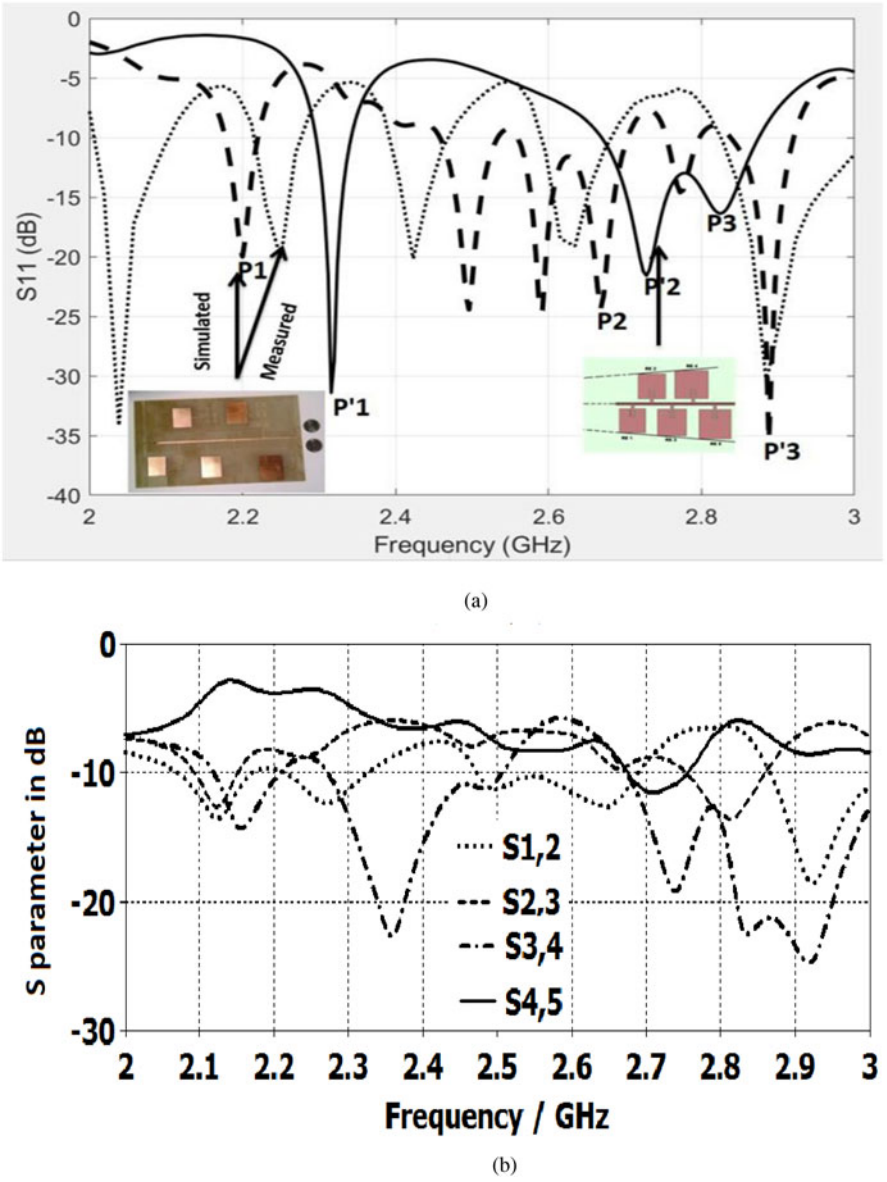


**Fig. 7.** *S*-parameter for five-element LPMA: (a) comparison of $S_{11}$ simulated (proposed and [3]) and measured and (b) simulated mutual coupling in the prototype.

for a log-periodic antenna. Moreover, this also prevents any chance of overlapping two successive patches.

The distance between the originating points of these branch lines on the main feed line ($D_k$) and each portion of the 90° bends ("$l_k$" and "$d_k$") obey the log-periodic scaling principle. So, we use the following formulae to find their length. The characteristic impedance of the mainline is 50 Ω, which gives its width. The branch line characteristic impedance is adjusted to transform the $k$th antenna element impedance to 50 Ω (i.e. mainline impedance) at frequency $f_k$:

$$d_k = \frac{c\tau^{k-1}}{4f_1\sqrt{\varepsilon_{eff,1}}} \tag{4}$$

$$l_k = \frac{c\tau^{k-1}}{2f_1\sqrt{\varepsilon_{eff,1}}} \tag{5}$$

$$D_k = \frac{c\tau^{k-1}}{2f_1\sqrt{\varepsilon_{eff,1}}} \tag{6}$$

## Design algorithm

The following is the design flow for an LPMA with scaling factor $\tau$, element bandwidth percentage $B$, lower frequency $f_l$, upper frequency $f_u$, number of elements $N$, and branch feedline width $w_b$:

(1) Read $B$, $f_l$, and $f_u$
(2) Assign $\tau$ randomly a value between 1 and 1.05
(3) Calculate $N$ using $f_u/f_1 = \tau^{1-N}$
(4) Calculate $f_k$ using $f_k/f_1 = \tau^{1-k}$, $k = 2$ to $N-1$
(5) Calculate the minimum number of elements ($N_{min}$) using equation (1)
(6) Calculate the dimension of each element using equations (2)–(6)
(7) Obtain width of $k$th branch line ($k = 1$ to $N$) to transform the impedance of $k$th element to 50 Ω.

## LPMA simulation and prototype

To test the proposed design method, the degree of resemblance between results from simulations and measurements on the

https://doi.org/10.1017/S1759078722000290 Published online by Cambridge University Press

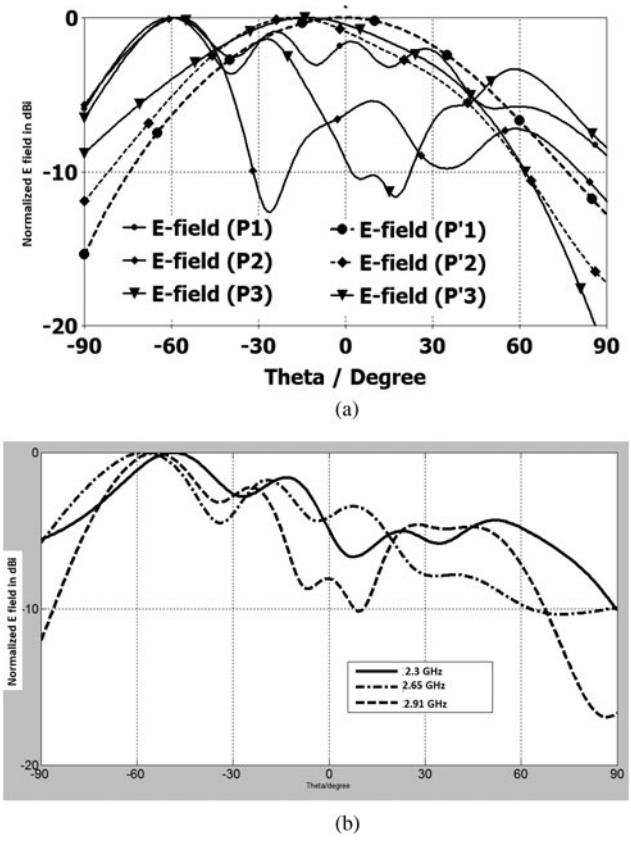


**Fig. 8.** *E*-plane radiation pattern: (a) comparison of simulated patterns and (b) measured with prototype.

prototype followed a comparison with the work of Gardener *et al.* [7] by reproducing their findings using electromagnetic simulation. The CST MWS, with 50 dB accuracy, was used to simulate and reproduce the results of Gardner *et al.* [7] for an LPMA which operates in the frequency range of 2.03–2.73 GHz (in the paper [7] $S_{11}$ plot is from 1 to 5 GHz). Assuming an optimistic bandwidth of 3% for each radiator, the minimum number of elements from equation (1) is three for this design. They had used seven and five elements which are well over this minimum value. The simulation preserved these numbers and other specifications (Table 1). A re-simulation followed with the proposed design without changing the specifications. As per the proposed design, the prototype (Fig. 2) was fabricated for testing the five-element LPMA due to constraints of available resources and facilities.

## Result and discussion

Table 2 shows the design parameters of the LPMAs with five (the shaded portion of the table) and seven elements. The square patch in [7] is for suppressing higher-order modes. The length is responsible for resonant frequency, so the side length of the square patch is close to that of the patch from the proposed method. However, due to the difference in the determination of dimensions, the lengths do not match. It results in mismatch of results from the two approaches, as evident from resonant peaks and return-loss plots (Fig. 3).

Figure 3 compares $S_{11}$ parameters for the seven-element LPMA in [7] with the proposed one. There are seven peaks in and around the desired band for the configuration of [7]. It can be due to the assumed principle that only the resonating element exists, under negligible mutual coupling, while design effectively open circuits others. The reason behind the other smaller peaks may be the weak mutual coupling, higher-order modes, and so forth. The lower peak is at 1.8 GHz, and the upper one is at 3.1 GHz instead of 2.03 and 2.73 GHz, respectively. It can be due to weak mutual coupling and excitation of orthogonal modes.

The proposed design also has seven peaks around the band of interest. Out of these, five are more prominent than those from [7]. Besides, there is also a small peak between the fourth and fifth peaks. Moreover, Fig. 4 shows the electric field distribution at 2.13, 2.66, and 2.77 GHz, which indicate the excitation of adjacent elements with the resonating one. These imply a not so weak mutual coupling effect, as in the case of [7] (Fig. 5).

Figure 6 compares the radiation patterns of both the LPMA designs at selected peaks. For our proposed model ($P1$, $P2$, $P3$, and $P4$), the main lobe is directed closer to the end-fire direction ($\theta = 90°$) than for the Gardner model ($P'1$, $P'2$, $P'3$, and $P'4$). The dip at $\theta = 90°$ is due to diffraction at the ground plane edge and will be characteristics of any end-fire antenna mounted on a finite ground plane. All patterns are linearly polarized. Thus, the proposed formulae and feed method take the design closer to true log-periodic characteristics while Gardner's fails to do so, as is evident from its non-end-fire radiation pattern. Figure 7 shows $S$ parameters of five-element LPMA. It compares (Fig. 7(a)) the $S_{11}$ of the fabricated prototype and simulated ones and looks at theoretical mutual coupling for the proposed LPMA (Fig. 7(b)). Contrary to the expectation, for the simulated Gardner-type LPMA, there are only three prominent peaks. It also shows a smaller bandwidth. It happens as the designs of the fourth and fifth (largest) elements are for the two lowest frequencies, and the reduced mutual coupling between the elements is insufficient for coverage of the complete band.

Moreover, due to this, adjacent elements of the main resonator could not be excited sufficiently to become active; so, the active region cannot move along the array elements. The last two elements are farthest from the first two but nearer to the third element. So, their presence affects the resonant frequency of the third element, which shifts downward from that of the second resonant frequency. It leads to a band notch of around 0.3 GHz between the second ($P'2$) and third ($P'1$) operating bands.

However, as expected, there are five resonant peaks in Fig. 7(a) for the proposed design (simulated and measured). The explanation for this is shown in Fig. 7(b). It shows the $S$-parameters between different elements. It indicates an appreciable coupling between, at least two neighboring antennas throughout the band of interest. This figure also shows that the measured $S_{11}$ closely follows the simulated one. This apparent behavior is due to three reasons: (1) fabrication tolerances in the prototype, while simulations are for ideal values; (2) electromagnetic interference (EMI) in the measurement environment due to unavailability of an anechoic chamber; and (3) four times expansion of the frequency axis compared to Fig. 3.

Nevertheless, the mismatch indicates obtaining the desired radiation pattern may not be possible. Figure 8 shows radiation patterns of the LPMA prototype for further discussion of this issue. As shown in Fig. 6, the traditional (i.e. Gardner) feed maintains a broadside pattern in the simulation (Fig. 8(a)). Both simulation and measurement results on the prototype

https://doi.org/10.1017/S1759078722000290 Published online by Cambridge University Press

**Table 3.** LPMA model comparison

| Antenna model (reference) | Direction of radiation (major lobe direction) | Elements in the array | Impedance bandwidth | Max gain (dBi) | Substrate used ($\varepsilon_r$) |
|---|---|---|---|---|---|
| [6] | Broad side | 5 | Multiband | 7.7 | FR4 (4.4) |
| [7] | Broad side | 5, 7 | Multiband | 6, 7.2 | FR4 (4.4) (sim.) |
| [8] | Broad side | 11 | 2.26–6.85 GHz | 10.3 | Teflon (2.65) |
| [10] | Broad side | 6 | 1.75–3 GHz | 6 | FR4 (4.4) |
| [11] | Broad side | 20 pairs | 2–6 GHz | 8.5 | RO4003C (3.38) |
| [12] | Broad side | 7 | 1–2.4 GHz | 7 | FR4 (4.4) |
| [13] | Broad side | 14 | 6.9–17.4 GHz | 9.95 | Rogers 5880 |
| Proposed antenna | End-fire | 5, 7 | 2.2–3 GHz | 9.8, 10.2 | FR4 (4.4) |

show that the *E*-plane radiation patterns are toward the end-fire direction.

Besides, the proposed design also shows out-of-band resonant peaks. These may be due to spurious radiation due to sharp bends and junctions in the branch line (particularly at lower frequencies below the dominant frequency of the largest patch). These may be mostly due to the excitation of higher-order modes at the upper end. Embedding suitable filters in the main feedline can suppress such spurious peaks. In [7], the design aims at radiation only from resonating elements by reducing their mutual coupling with neighboring elements.

## Conclusion

This study developed a design technique for LPMAs to operate like LPDAs. It considered characteristics of LPDAs and compared them with different pre-existing LPMA designs (Table 3). Analyzing differences in characteristics, new LPMA designs gradually evolved until obtaining a satisfactory design. In the final design, LPMA elements have a common axis of alignment with appropriate feeding so that the phase difference between the two consecutive elements is 180°. The final design gives an almost end-fire pattern ($\theta \approx 70°$) with a gain of 9.8 dBi. In the 2.2–3 GHz range, the fabricated prototype of five elements shows four resonant peaks (2.23, 2.45, 2.65, and 2.91 GHz) with errors of (1.34, 2.4, 1.52, and 0.35%) compared to simulated results. The differences between the measured and simulated results can be due to the measurement and fabrication tolerances, and unavailability of the anechoic chamber for measurement. As this antenna exhibits a gain of 9.8 dBi with impendence bandwidth from 2.2 to 3 GHz, it is suitable for Bluetooth, ZigBee, wireless LANs, and satellite radio communication.

## References


1. **Smith CE** (1966) *Log Periodic Antenna Design Handbook*, 1st Edn. Cleveland, Ohio: Smith Electronics, Inc.
2. **DuHamel RH and IsBell DE** (1957) Broadband logarithmically periodic antenna structures. *IRE National Convention Record, Part I* **5**, 119–128.
3. **IsBell DE** (1960) Log periodic dipole arrays. *IRE Transactions on Antennas and Propagation* **AP-8**, 260–267.
4. **Carrel RL** (1961) The design of log-periodic dipole antennas. *IRE National Convention Record, Part I* **9**, 61–75.
5. **Pues H, Bogaer J, Pieck R and Van De Capelle A** (1981) Wideband quasi log-periodic microstrip antenna. *IEE Proceedings H (Microwaves, Optics and Antenna* **128**, 159–163.
6. **Dadel M and Srivastava S** (2011) Arrays of patch antenna using log periodic property. *IEEE International RF and Microwave Conference (RFM)*. doi: 10.1109/RFM.2011.6168768.
7. **Rahim MKA and Gardner P** (2003) Microstrip log periodic antenna using circuit simulator. *Proceedings of 6th International Symposium on Antennas, Propagation and EM Theory*, pp. 202–205. http://ieeexplore.ieee.org/stamp/stamp.jsp?tp=&arnumber=1276663
8. **Wu Q, Jin R and Geng J** (2010) A single-layer ultrawideband microstrip antenna. *IEEE Transactions on Antennas and Propagation* **58**, 211–214.
9. **Chen Q, Wu W, Di Y and Hu Z** (2018) A planar compact helical log-periodic array. *IEEE International Symposium on Antennas and Propagation & USNC/URSI National Radio Science Meeting, Boston, MA*, pp. 845–846. doi: 10.1109/APUSNCURSINRSM.2018.8609241.
10. **Anagnostou DE, Papapolymerou J, Christodoulou CG and Tentzeris M** (2006) A small planar log-periodic Koch-dipole antenna (LPKDA). *IEEE Antennas and Propagation Society International Symposium, Albuquerque, NM*, pp. 3685–3688. doi: 10.1109/APS.2006.1711421.
11. **Zengin F** (2019) The effects of the trapezoidal dipole array elements on planar log periodic antenna. *IEEE-APS Topical Conference on Antennas and Propagation in Wireless Communications (APWC), Granada, Spain*, pp. 333–336.
12. **Rajendran J and Menon SK** (2016) A low-cost compact wideband printed planar log periodic Sierpinski antenna. *Progress in Electromagnetic Research Symposium* (*PIERS*), vol. 1, No. 1, pp. 2752–2756. doi: 10.1109/PIERS.2016.7735117.
13. **Hu Z, Cao S, Liu M, Hua C and Chen Z** (2019) A planar low-profile log-periodic array based on cavity-backed slot. *IEEE Antennas and Wireless Propagation Letters* **18**, 1966–1970.
14. **Chen L and Hong J** (2018) A novel log-periodic MIMO antenna for UWB system. *International Conference on Microwave and Millimeter Wave Technology* (*ICMMT*), pp. 1–3. doi: 10.1109/ICMMT.2018.8563307.
15. **Surjati I, Alam S and Ningsih YK** (2018) Increasing bandwidth of log periodic array microstrip antenna using parasitic air gap for digital video broadcasting application. *4th International Conference on Wireless and Telematics (ICWT)*, pp. 1–5. doi: 10.1109/ICWT.2018.8527828.
16. **Hall PS** (1986) Multioctave bandwidth log periodic microstrip antenna array. *IEE Proceedings H (Microwaves, Optics and Antenna* **133**, 127–136.
17. **Mishra RK** (2013) Transmission line model for log periodic microstrip antenna. *Presented at IEEE AP-s International Symposium*. [Online]. Available at http://ieeexplore.ieee.org/stamp/stamp.jsp?arnumber=6710745.
18. **Muduli A and Mishra RK** (2017) Transmission line model for a series fed log-periodic microstrip antenna array. *IEEE INDICON-2017, IIT Roorkee, 15–17 Dec 2017, Roorkee, India* [Online]. Available at https://ieeexplore.ieee.org/document/8487696.
19. **Ji F, Wang Z, Nie L and Jiang Z** (2020) A design of microstrip log periodic antenna unit. *Cross Strait Radio Science & Wireless Technology Conference (CSRSWTC)*, pp. 1–3. doi: 10.1109/CSRSWTC50769.2020.9372594.
20. **Roges R, Malik PK and Sharma S** (2021) A compact CPW-fed log-periodic antenna for IoT applications. *International Conference on*


https://doi.org/10.1017/S1759078722000290 Published online by Cambridge University Press

*Communication, Control and Information Sciences (ICCISc)*, pp. 1–5. doi: 10.1109/ICCISc52257.2021.9484975.

**Arjuna Muduli** was born in India in 1985. He is an associate professor in the Department of Electronics and Communication Engineering at KLEF (Deemed to be University), Vijayawada, AP-522502, India. He has received his Ph.D. degree from Berhampur University, Odisha. His research interest includes RF and antennas, wireless communication, software-defined radios, and cognitive radios. He worked as a DST INSPIRE fellow (Govt. of India) from 2011 to 2016. He qualified UGC NET (Govt. of India) in 2012. He has received Gold Medal for acquiring first position in both M.Tech. and M.Sc. programs. He is a fellow of IETE, India and a senior member of IEEE.

**Rabindra K. Mishra** was born in India in 1963. He is a professor in the Electronic Science Department of Berhampur University. He has researched extensively in the areas of planar antennas and applications of soft-computing techniques for analysis and design of planar antennas. He had visited the University of Birmingham as a British Commonwealth Fellow during 1999–2000. He has supervised 10 doctoral theses. He has published two monographs and over 150 learned articles in journals of repute and proceedings of conferences, seminars, etc. These publications have earned the IETE Sir J. C. Bose best application paper award (1999), Shri Hari Ohm Ashram Prerit Hariballabha Das Chunilal Research Endowment Award (2000), and Samanta Chandra Sekhar Award in Engineering & Technology (2008), which is the highest award by the Govt. of Odisha.

https://doi.org/10.1017/S1759078722000290 Published online by Cambridge University Press